

# Evaluation of the Outcome of Lung Nodules Missed on $^{18}\text{F}$ -FDG PET/MRI Compared with $^{18}\text{F}$ -FDG PET/CT in Patients with Known Malignancies

Lino M. Sawicki<sup>1</sup>, Johannes Grueneisen<sup>2</sup>, Christian Buchbender<sup>1</sup>, Benedikt M. Schaarschmidt<sup>1</sup>, Benedikt Gomez<sup>3</sup>, Verena Ruhlmann<sup>3</sup>, Lale Umutlu<sup>2</sup>, Gerald Antoch<sup>1</sup>, and Philipp Heusch<sup>1</sup>

<sup>1</sup>Department of Diagnostic and Interventional Radiology, Medical Faculty, University Dusseldorf, Dusseldorf, Germany;

<sup>2</sup>Department of Diagnostic and Interventional Radiology and Neuroradiology, Medical Faculty, University Duisburg-Essen, Essen, Germany; and <sup>3</sup>Department of Nuclear Medicine, Medical Faculty, University Duisburg-Essen, Essen, Germany

The lower detection rate of  $^{18}\text{F}$ -FDG PET/MRI than  $^{18}\text{F}$ -FDG PET/CT regarding small lung nodules should be considered in the staging of malignant tumors. The purpose of this study was to evaluate the outcome of these small lung nodules missed by  $^{18}\text{F}$ -FDG PET/MRI. **Methods:** Fifty-one oncologic patients (mean age  $\pm$  SD, 56.6  $\pm$  14.0 y; 29 women, 22 men; tumor stages, I [ $n$  = 7], II [ $n$  = 7], III [ $n$  = 9], IV [ $n$  = 28]) who underwent  $^{18}\text{F}$ -FDG PET/CT and subsequent  $^{18}\text{F}$ -FDG PET/MRI on the same day were retrospectively enrolled. Images were analyzed by 2 interpreters in random order and separate sessions with a minimum of 4 wk apart. A maximum of 10 lung nodules was identified for each patient on baseline imaging. The presence, size, and presence of focal tracer uptake was noted for each lung nodule detected on  $^{18}\text{F}$ -FDG PET/CT and  $^{18}\text{F}$ -FDG PET/MRI using a postcontrast T1-weighted 3-dimensional gradient echo volume-interpolated breath-hold examination sequence with fat suppression as morphologic dataset. Follow-up CT or  $^{18}\text{F}$ -FDG PET/CT (mean time to follow-up, 11 mo; range, 3–35 mo) was used as a reference standard to define each missed nodule as benign or malignant based on changes in size and potential new tracer uptake. Nodule-to-nodule comparison between baseline and follow-up was performed using descriptive statistics. **Results:** Out of 134 lung nodules found on  $^{18}\text{F}$ -FDG PET/CT,  $^{18}\text{F}$ -FDG PET/MRI detected 92 nodules. Accordingly, 42 lung nodules (average size  $\pm$  SD, 3.9  $\pm$  1.3 mm; range, 2–7 mm) were missed by  $^{18}\text{F}$ -FDG PET/MRI. None of the missed lung nodules presented with focal tracer uptake on baseline imaging or follow-up  $^{18}\text{F}$ -FDG PET/CT. Thirty-three out of 42 missed lung nodules (78.6%) in 26 patients were rated benign, whereas 9 nodules (21.4%) in 4 patients were rated malignant. As a result, 1 patient required upstaging from tumor stage I to IV. **Conclusion:** Although most small lung nodules missed on  $^{18}\text{F}$ -FDG PET/MRI were found to be benign, there was a relevant number of undetected metastases. However, in patients with advanced tumor stages the clinical impact remains controversial as upstaging is usually more relevant in lower stages.

**Key Words:** lung; nodules; MRI; PET/MRI; PET/CT

**J Nucl Med** 2016; 57:15–20

DOI: 10.2967/jnumed.115.162966

**M**etastatic spread to the lungs commonly implies a higher tumor stage in patients with malignant diseases often requiring a change of therapy regimen and ultimately decreasing chances of survival (1). Hence, the early detection of potential pulmonary metastases is essential. Because of a higher accuracy in TNM staging than either PET or CT alone (2), integrated  $^{18}\text{F}$ -FDG PET/CT has been implemented in the staging routine of a growing number of tumor entities and is regarded as the standard of reference by many authors (3–5). MRI, on the other hand, offers a sensitivity superior to that of CT concerning infiltration of the primary tumor into adjacent organs and detection of metastasis to parenchymatous organs such as the liver, brain, or kidneys (6–8). In addition, MRI provides valuable functional information from quantitative and multiparametric imaging (9). With the introduction of fully integrated PET/MRI systems, PET and MRI can be used synergistically in a single modality, taking advantage of an exact correlation between  $^{18}\text{F}$ -FDG-avid lesions and the anatomic details obtained by MR images (10–12). Yet, regarding lung imaging, even when using high spatial resolution T1-weighted (T1w) 3-dimensional (3D) gradient echo (GRE) sequences (e.g., volume-interpolated breathhold-examination [VIBE]) recommended for the identification of small pulmonary nodules (13–15), PET/MRI seems to be outmatched by PET/CT (16). Underlying reasons are found in PET/MRI's lower sensitivity regarding  $^{18}\text{F}$ -FDG-negative lesions (17,18) because of a low proton density in aerated lungs, fast decay of signal caused by susceptibility artifacts at air–tissue boundaries, and motion artifacts caused by breathing and cardiac pulsation. Bearing in mind the increasing use of whole-body PET/MRI, its lower detection rate of small lung nodules potentially representing metastases should be considered in the staging of malignant tumors. Hence, the purpose of this study was to evaluate the outcome of small lung nodules detected on  $^{18}\text{F}$ -FDG PET/CT but missed by  $^{18}\text{F}$ -FDG PET/MRI in terms of their presumed dignity.

## MATERIALS AND METHODS

### Patients and Inclusion Criteria

Patients with a known malignancy (Table 1) who underwent  $^{18}\text{F}$ -FDG PET/MRI including a postcontrast, fat-suppressed (fs) T1w VIBE sequence of the thorax after clinically indicated  $^{18}\text{F}$ -FDG PET/CT for tumor staging on the same day were retrospectively enrolled in this study. A follow-up CT or  $^{18}\text{F}$ -FDG PET/CT not less than 3 mo after the initial examination had to be available for outcome evaluation. According to these criteria, 51 patients (mean age  $\pm$  SD, 56.6  $\pm$  14.0 y; 29 women,

Received Jul. 16, 2015; revision accepted Sep. 8, 2015.

For correspondence or reprints contact: Lino Sawicki, University Dusseldorf, Medical Faculty, Department of Diagnostic and Interventional Radiology, Moorenstrasse 5, D-40225 Dusseldorf, Germany.

E-mail: linomorris.sawicki@med.uni-duesseldorf.de

Published online Oct. 29, 2015.

COPYRIGHT © 2016 by the Society of Nuclear Medicine and Molecular Imaging, Inc.

22 men) between May 2012 and December 2014 were eligible for retrospective analysis. The study cohort comprised patients with tumor stages I ( $n = 7$ ), II ( $n = 7$ ), III ( $n = 9$ ), and IV ( $n = 28$ ). Eight out of 51 patients had a recurrent malignancy. The study was approved by the local ethics committee, and all subjects signed an informed consent form.

### PET/CT Imaging

Patients underwent whole-body (i.e., head to upper thighs)  $^{18}\text{F}$ -FDG PET/CT on a Biograph mCT or Biograph Duo (Siemens Healthcare GmbH)  $61 \pm 8$  min after intravenous injection of a mean activity of  $260 \pm 60$  MBq of  $^{18}\text{F}$ -FDG, depending on their body weights. At injection time, blood glucose levels needed to be below 150 mg/dL. Twenty-three patients were examined using the low-dose CT technique. In 28 patients, full-dose CT scans were obtained. Full-dose CT scans were acquired after intravenous injection of a contrast agent (Imeron 300; Bracco Imaging Deutschland GmbH). In all full-dose PET/CT scans, an additionally acquired dedicated lung scan applying a sharp b 70 or b 90 kernel in deep inspiration was used for the detection of lung nodules. CT images were displayed on lung window setting and using a slice thickness of 2 mm. For dose-reduction purposes, the manufacturer-supplied solutions CareKV and CareDose 4D (Siemens Healthcare GmbH) were used for both full- and low-dose PET/CT scans (presets: 120 kV, 210mAs and 120 kV, 40 mAs, respectively). PET acquisition time using static frames varied from 2 to 3.5 min per bed position. Iterative reconstruction (3 iterations, 21 subsets) with a gaussian filter of 4.0 mm was applied. In general, the slice thickness of reconstructed PET images was 3 mm. For attenuation correction of the PET dataset, the portal venous phase of full-dose CT scans and low-dose CT data in low-dose scans were used.

### PET/MR Imaging

Whole-body (i.e., head to upper thighs)  $^{18}\text{F}$ -FDG PET/MRI using Flex coils (Siemens Healthcare AG GmbH) was performed on a 3-T Biograph mMR (Siemens Healthcare AG). The average delay after intravenous tracer injection was  $117 \pm 29$  min. For morphologic assessment of the lungs, a transverse T1w fs VIBE sequence (repetition time, 4.08 ms; echo time, 1.51 ms; slice thickness, 3.5 mm; field of view,  $400 \times 300$  mm; matrix size,  $512 \times 307.2$ ; voxel size,  $1.3 \times 0.8 \times 3.5$  mm) after contrast administration (Dotarem; Guerbet GmbH) was acquired. Attenuation correction was based on a coronal 3D Dixon-VIBE sequence (repetition time, 3.6 ms; echo time 1, 1.23 ms; echo time 2, 2.46 ms; slice thickness, 3.12 mm; field of view,  $500 \times 328$  mm; matrix size,  $192 \times 121$  mm; voxel size,  $4.1 \times 2.6 \times 3.1$  mm). In general, PET acquisition time was 3 min per bed position. PET images were acquired in list-mode and reconstructed using an iterative algorithm of ordered-subsets expectation maximization (3 iterations and 21 subsets). A gaussian filter of 4.0 mm was applied. In general, the slice thickness of reconstructed PET images was 3 mm.

### Follow-up Imaging

Chest CT ( $n = 32$ ) and whole-body  $^{18}\text{F}$ -FDG PET/CT ( $n = 19$ ) scans were considered appropriate for follow-up imaging and categorization of dignity of the missed lung nodules. Follow-up CT examinations were conducted on 1 of the following CT scanners: Definition AS+, Definition Flash, and Definition Force (Siemens Healthcare GmbH). Follow-up  $^{18}\text{F}$ -FDG PET/CT examinations were performed on the aforementioned Biograph mCT or Biograph Duo (Siemens Healthcare AG). Baseline and follow-up examinations had to be a minimum of 3 mo apart. For follow-up imaging, the most recent CT or  $^{18}\text{F}$ -FDG PET/CT scan was selected. The average follow-up interval was  $11 \pm 8$  mo (range, 3–35 mo). Table 2 gives an overview of patient numbers and tumor types in different follow-up intervals.

### Image Analysis

Images were evaluated on a dedicated OsiriX Workstation (Pixmeo SARL). Baseline  $^{18}\text{F}$ -FDG PET/CT and  $^{18}\text{F}$ -FDG PET/MRI datasets as well as follow-up CT or  $^{18}\text{F}$ -FDG PET/CT scans were analyzed by 2 independent radiologists with 3 and 5 y of experience in hybrid imaging. Interpreters were aware of patients' diagnosis. Any discrepancies between the 2 interpreters were resolved in a subsequent consensus reading. PET images were reviewed with and without attenuation correction of the PET data to prevent false-positive findings caused by attenuation-correction artifacts. Baseline  $^{18}\text{F}$ -FDG PET/CT and  $^{18}\text{F}$ -FDG PET/MRI were assessed in random order and in separate sessions with a minimum of 4 wk apart to avoid recognition bias. Morphologic T1w fs VIBE and CT images and PET from PET/CT and PET from PET/MRI were analyzed separately and as fused datasets. The presence, size (i.e., longitudinal axis diameter on transverse images) on the CT component of  $^{18}\text{F}$ -FDG PET/CT, and presence of focal tracer uptake above surrounding background was noted for each lung nodule detected on  $^{18}\text{F}$ -FDG PET/CT and on  $^{18}\text{F}$ -FDG PET/MRI. Initially, a maximum of 10 lung nodules was identified for each patient on baseline imaging, beginning with the right upper lobe proceeding to the left lower lobe. Each lung nodule found on  $^{18}\text{F}$ -FDG PET/CT but not detected on  $^{18}\text{F}$ -FDG PET/MRI was rated a missed nodule. In a separate session, the size of each missed lung nodule was reassessed on follow-up CT or  $^{18}\text{F}$ -FDG PET/CT, respectively. In cases, in which a PET/CT scan was available for follow-up, missed nodules were also analyzed in regard to a potential new  $^{18}\text{F}$ -FDG uptake.

### Standard of Reference

Because histopathologic correlation could not be obtained for any of the missed lung nodules, the standard of reference to determine the outcome of a missed lung nodule was based on change in nodule size between baseline and follow-up imaging (chest CT or  $^{18}\text{F}$ -FDG PET/CT) and presence of new  $^{18}\text{F}$ -FDG avidity of a lung nodule on follow-up PET/CT.

Potential systemic therapy was addressed as follows: nodules presenting smaller on follow-up were rated malignant if the patient underwent systemic cancer therapy during the time of follow-up (i.e., therapy effect) or rated benign provided no cancer therapy had been administered. Nodules presenting constant in size were rated benign, regardless of whether the patient received cancer therapy or not. This procedure for nodules constant in size was decided on to avoid overestimation of the number of metastases while acknowledging that the overall number of metastases may have been underestimated by this approach. Nodules with an increased size on follow-up or a new  $^{18}\text{F}$ -FDG avidity on follow-up PET/CT were rated malignant (Fig. 1).

### Statistics

SPSS Statistics 22 (IBM) was used for statistical analysis. All data are mean  $\pm$  SD. Descriptive analysis was used for the calculation of the patients' characteristics and for follow-up nodule-to-nodule comparison. Similar to previous reports (19), reliability between interpreters was performed in a descriptive way.

**TABLE 1**

Tumor Entities Within Study Cohort Sorted by Frequency

Tumor	<i>n</i>
Lung cancer	12
Breast cancer	8
Ovarian cancer	7
Lymphoma	5
Gastrointestinal cancer	3
Malignant melanoma	3
Malignant mesothelioma	3
Other (<3 cases/entity)	10

**TABLE 2**  
Tumor Entities in 3 Different Follow-up Intervals Sorted by Frequency

3–6 mo (n)	6–12 mo (n)	>12 mo (n)
Lung cancer (10)	Ovarian cancer (4)	Colorectal cancer (2)
Breast cancer (5)	Breast cancer (3)	Ovarian cancer (2)
Lymphoma (3)	Lung cancer (2)	Malignant melanoma (2)
Sarcoma (2)	Lymphoma (2)	Uterine cancer (1)
Mesothelioma (2)	Mesothelioma (1)	Head and neck cancer (1)
Ovarian cancer (1)	Sarcoma (1)	
Uterine cancer (1)	Thyroid cancer (1)	
Thyroid cancer (1)	Cervical cancer (1)	
Cholangiocellular cancer (1)	Malignant melanoma (1)	
Total = 26	Total = 17	Total = 8

## RESULTS

There was 97% agreement between both interpreters on all lung nodules detected by  $^{18}\text{F}$ -FDG PET/CT and  $^{18}\text{F}$ -FDG PET/MRI, with only 3% needing a consensus reading, in which agreement was found in all cases. In 51 patients, 134 lung nodules were found on  $^{18}\text{F}$ -FDG PET/CT (mean size,  $12.9 \pm 15.7$  mm; range, 2–98 mm; lung nodules per patient, 0–10).  $^{18}\text{F}$ -FDG PET/MRI detected 92 of these lung nodules, signifying a detection rate of 68.7%.  $^{18}\text{F}$ -FDG PET/MRI and  $^{18}\text{F}$ -FDG PET/CT detected concordant numbers of lung nodules in 21 patients, 9 of which did not exhibit any lung nodules. In the other 30 patients, 42 lung nodules were missed on  $^{18}\text{F}$ -FDG PET/MRI but detected on  $^{18}\text{F}$ -FDG PET/CT (Fig. 2). The percentage of missed nodules with respect to the total number of lung nodules was 31.3%. The mean size of the missed nodules was  $3.9 \pm 1.3$  mm (range, 2–7 mm) (Fig. 3). On average, 0.8 pulmonary nodules per patient were missed on  $^{18}\text{F}$ -FDG PET/MRI compared with  $^{18}\text{F}$ -FDG PET/CT. None of the missed lung nodules presented with focal  $^{18}\text{F}$ -FDG uptake above the surrounding background on baseline attenuation-corrected or non-attenuation-corrected PET images. Nodule-to-nodule follow-up assessment revealed that 71.4% (30/42) of missed lung nodules remained constant in size, 26.2% (11/42) of missed lung nodules decreased in size or completely resolved, and 2.4% (1/42) of lung nodules increased in size on follow-up CT or  $^{18}\text{F}$ -FDG PET/CT compared with baseline imaging. None of

the missed lung nodules demonstrated a new tracer uptake on follow-up  $^{18}\text{F}$ -FDG PET/CT. Seventy percent (21/30) of the patients with missed lung nodules received systemic or local cancer therapy in the interval of baseline PET/MRI or PET/CT and follow-up CT or  $^{18}\text{F}$ -FDG PET/CT, whereas 30% (9/30) of the patients were not subjected to cancer therapy. According to the reference standard, 78.6% (33/42) of the missed pulmonary nodules in 26 out of 30 (86.7%) patients were rated benign, whereas 21.4% (9/42) of the missed pulmonary nodules in 4 out of 30 (13.3%) patients were rated malignant (Figs. 4 and 5). Because of the occurrence of a new metastatic spread to the right lung, upstaging from tumor stage I to tumor stage IV was required in 1 of the 4 patients. This patient was initially diagnosed with a T1 N0 M0 non-small cell lung cancer in the contralateral lung. As a consequence, the contralateral lung metastasis demanded restaging to M1a (20). Because distant metastases had already been diagnosed in the other 3 patients, no adjustment of TNM staging was necessary in these cases.

## DISCUSSION

The intention of this study was to evaluate the outcome of small lung nodules detected on  $^{18}\text{F}$ -FDG PET/CT, which were not identifiable on  $^{18}\text{F}$ -FDG PET/MRI in oncologic patients. According to the reference standard, most (78.6%) of these missed lung nodules were rated as benign but there was a small but relevant number (21.4%) of undetected lung nodules that were suggestive of metastases.

The detection of small lung nodules is a key clinical demand in cancer staging because potential metastatic spread can have far-reaching effects on therapy and patient survival (1,13,20). Today, whole-body  $^{18}\text{F}$ -FDG PET/CT is widely available and used not only to identify lung nodules but also to discriminate malignant from benign pulmonary masses, enabling a comprehensive tumor staging in a 1-stop shop examination (21–23). On the other hand, the latest transition from a mere research modality into clinical practice raised issues regarding the eligibility of  $^{18}\text{F}$ -FDG PET/MRI to detect small pulmonary nodules compared with CT or PET/CT as the modality of choice for lung imaging.

None of the missed lung nodules, including those that were suggestive of metastasis, presented with a focal tracer uptake on the PET component of  $^{18}\text{F}$ -FDG PET/CT or  $^{18}\text{F}$ -FDG PET/MRI. However, given the fact that 21.4% of non- $^{18}\text{F}$ -FDG-avid nodules were likely malignant, our results indicate that PET negativity is not suitable

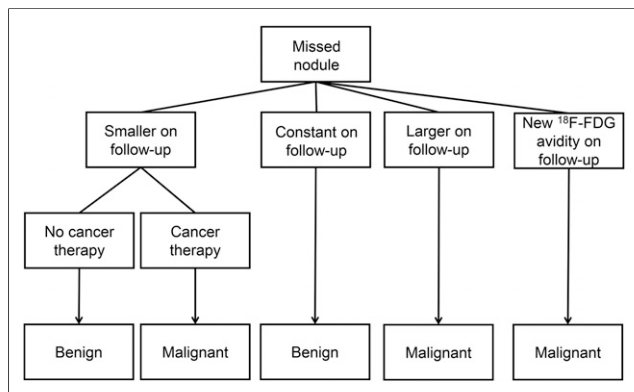


**FIGURE 1.** Flowchart to determine outcome of lung nodules missed by  $^{18}\text{F}$ -FDG PET/MRI.

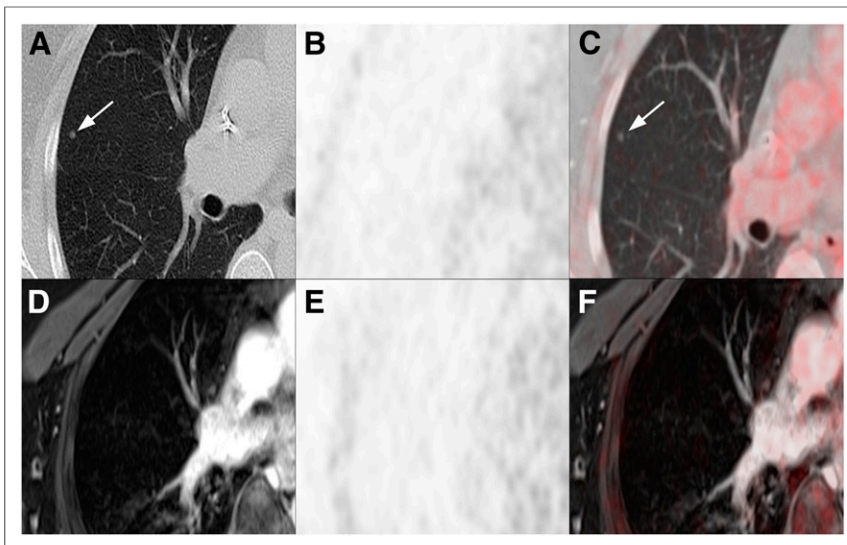


**FIGURE 2.** Images of a 50-y-old female patient with breast cancer. Five-millimeter lung nodule located in right upper lobe (arrows in A and C) identified on the CT images (A) of  $^{18}\text{F}$ -FDG PET/CT (E) but not recognizable on T1w fs VIBE images (D) of  $^{18}\text{F}$ -FDG PET/MRI (F). There was no corresponding  $^{18}\text{F}$ -FDG uptake on PET from PET/CT (B) and on PET from PET/MRI (E).

to rule out malignancy in small lung lesions. Studies by Yilmaz et al., Farid et al., and Khalaf et al. demonstrating a high prevalence of PET negativity in malignant nodules less than 1 cm have corroborated these results (24–26). False-negative findings might have been attributed to breathing motion, low metabolic activity (27), small nodule size, and the limited spatial resolution of PET, leading to a substantial underestimation of the true activity within the lesion (8). Moreover, differences between  $^{18}\text{F}$ -FDG PET/MRI and  $^{18}\text{F}$ -FDG PET/CT regarding PET reconstruction parameters—for instance, slice thickness—can influence nodule detectability of the PET component. With a slice thickness of around 3 mm for PET from  $^{18}\text{F}$ -FDG PET/MRI and from  $^{18}\text{F}$ -FDG PET/CT, both PET components can be regarded equally prone to partial-volume effects in our study. However, considering that a relevant proportion of nodules were 3 mm or less in size partial-volume effects might have been a relevant factor.

From the variety of clinically used MR sequences of the thorax, T1w 3D GRE sequences such as VIBE offer the highest detection rates of small pulmonary nodules and thus served as the only morphologic dataset in this study (13–15,28–30). Performed in a comparatively short imaging time ( $\sim 20$  s), they allow for an acquisition during breath-hold with accurate fusion of simultaneously acquired PET signals (31). Further advantages encompass high spatial resolution offering high-quality depiction of lung anatomy and a lower rate of artifacts compared with 2-dimensional GRE sequences (32). However, comparative studies examining the sensitivity of MRI and CT for lung nodules less than 1 cm found that MRI still lags behind CT, with detection rates ranging between 80% and 90% (14,17,30,33). Signal loss because of cardiac pulsation and respiration, susceptibility artifacts arising from multiple air-tissue interfaces, and low proton density in aerated lungs are known drawbacks hampering the identification of small pulmonary nodules (34). With a detection rate of approximately 70% for lung nodules less than 0.7 cm, our results seem to support these prior investigations.

Out of 4 patients with lung metastases missed by  $^{18}\text{F}$ -FDG PET/MRI, 2 patients had lung cancer and 2 had breast cancer, entities renowned for a high potential of developing lung metastases and thus further substantiating the suspicion of malignancy (35,36). However, because in 3 of the 4 patients distant metastases had already been diagnosed, a missed metastatic spread to the lungs should not be expected to have high therapeutic significance. A clinically relevant upstaging from tumor stage I to IV was required in only 1 of the patients. For all other patients with lung nodules missed by  $^{18}\text{F}$ -FDG PET/MRI, no adjustment of TNM staging was required. Given that most missed lung nodules proved benign and upstaging seemed to be necessary only in exceptional cases, from a clinical standpoint our results may generally endorse the use of whole-body  $^{18}\text{F}$ -FDG PET/MRI in oncologic patients. Nevertheless, this is partly due to study-specific patient characteristics, which mainly included patients with very advanced tumor stages. The evaluation of consequences on treatment decisions and prognosis might be addressed in future projects.

This study has some limitations. One limitation was the small and heterogeneous patient cohort comprising different tumor entities with a varying degree of metastatic potential and  $^{18}\text{F}$ -FDG avidity. The use of 2 different PET/CT protocols (1 with additional low-dose CT of the chest in maximal inspiration, 1 without) may have led to underestimation of the overall number of pulmonary nodules on the reference standard. Adding a low-dose CT in maximal inspiration should be a prerequisite when designing a follow-up study addressing a potential effect of missed pulmonary metastases on patient management. Also, the slice thickness of the CT component of baseline  $^{18}\text{F}$ -FDG PET/CT was 2 mm, whereas the slice thickness of T1w fs VIBE of  $^{18}\text{F}$ -FDG PET/MRI was 3.5 mm. Bearing in mind that missed lung nodules measured around 4 mm, the larger slice thickness of T1w fs VIBE might have contributed to the inferior detection rate of  $^{18}\text{F}$ -FDG PET/MRI. However, T1w VIBE images

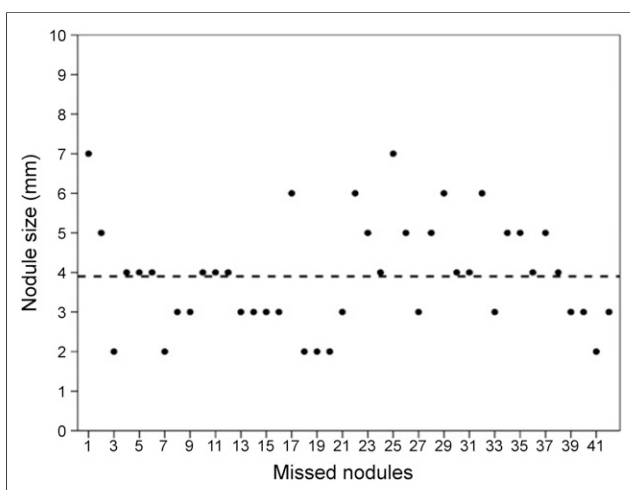


**FIGURE 3.** Sizes of 42 missed lung nodules measured on  $^{18}\text{F}$ -FDG PET/CT. Average size of nodules was 3.9 mm (broken line). Minimum and maximum sizes were 2 and 7 mm, respectively.

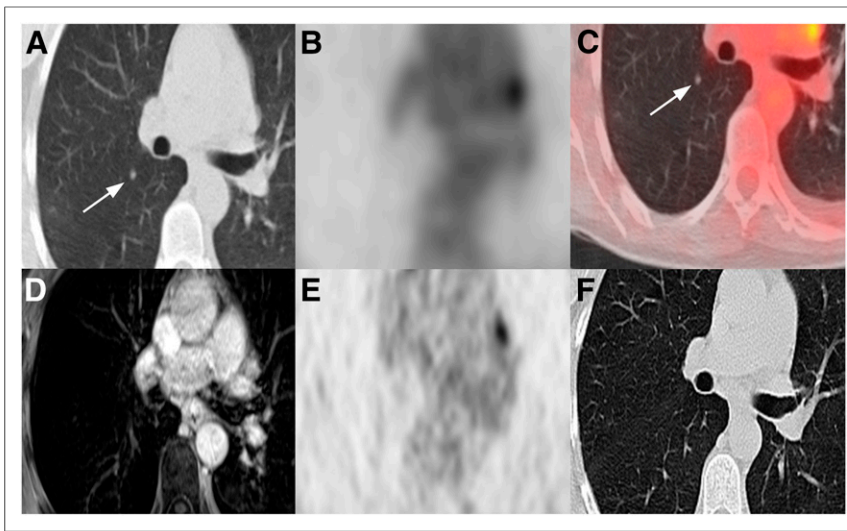


**FIGURE 4.** A 47-y-old female patient with breast cancer. Five-millimeter lung nodule located in right lower lobe (arrows in A and C) identified on CT component (A) of  $^{18}\text{F}$ -FDG PET/CT images (C) but not detectable on T1w fs VIBE images (D) of  $^{18}\text{F}$ -FDG PET/MRI. No focal  $^{18}\text{F}$ -FDG uptake was seen on PET from PET/CT (B) and PET from PET/MRI (E). After chemotherapy, 3-mo follow-up CT revealed complete disappearance of nodule (F). Note focal  $^{18}\text{F}$ -FDG uptake attributable to left hilar lymph node metastasis (B, C, and E).

of the chest are not yet feasible with a lower slice thickness than 3.5 mm. It could be assumed that the MRI component might have performed better using a lower slice thickness. However, technical requirements are yet to be introduced into clinical routine. It also has to be considered that a minor part of lung nodules presenting smaller in patients undergoing cancer therapy might still have been of infectious origin. In this case, the number of missed metastases may have been overestimated. Furthermore, some of the nodules that remained constant in size on follow-up might have represented metastases with partial response to systemic or local cancer therapy. Although the mean follow-up interval was 11 mo, many patients had follow-up intervals of less than 6 mo. In slowly growing lesions, one might argue that it was difficult to exclude false-negative readings. Lacking a histopathologic reference standard, these limitations have to be kept in mind when interpreting the results of this study.

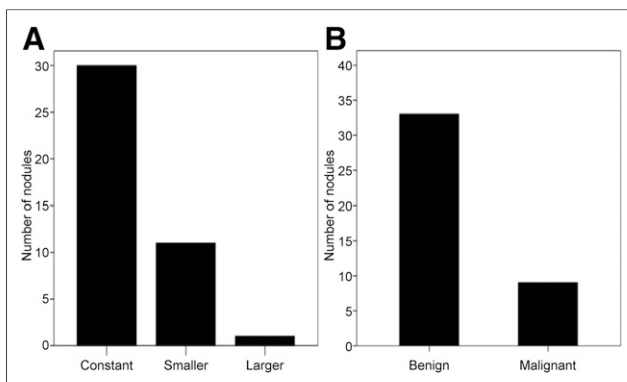


**FIGURE 5.** Development of nodule size comparing baseline and follow-up images (A). Outcome of lung nodules according to the standard of reference (B).

## CONCLUSION

Because of its lower sensitivity in detecting PET-negative lung nodules, whole-body  $^{18}\text{F}$ -FDG PET/MRI using a T1w VIBE sequence misses a relevant proportion of small lung nodules in oncologic patients. Although most missed lung nodules proved to be benign, there are a considerable number of metastases among those missed nodules. However, in patients with very advanced tumor stages the clinical impact remains controversial because potential upstaging is usually more relevant in lower tumor stages.

## DISCLOSURE

The costs of publication of this article were defrayed in part by the payment of page charges. Therefore, and solely to indicate this fact, this article is hereby marked “advertisement” in accordance with 18 USC section 1734. No potential conflict of interest relevant to this article was reported.

## REFERENCES

- Barth A, Wanek LA, Morton DL. Prognostic factors in 1,521 melanoma patients with distant metastases. *J Am Coll Surg.* 1995;181:193–201.
- Antoch G, Vogt FM, Freudenberg LS, et al. Whole-body dual-modality PET/CT and whole-body MRI for tumor staging in oncology. *JAMA.* 2003;290:3199–3206.
- Weber WA, Grosu AL, Czernin J. Technology insight: advances in molecular imaging and an appraisal of PET/CT scanning. *Nat Clin Pract Oncol.* 2008;5:160–170.
- Collins CD. PET/CT in oncology: for which tumors is it the reference standard? *Cancer Imaging.* 2007;7 Spec No A:S77–87.
- von Schulthess GK, Steinert HC, Hany TF. Integrated PET/CT: current applications and future directions. *Radiology.* 2006;238:405–422.
- Reiser M, Wiesmann W, Erlemann R, et al. Computerized tomography and magnetic resonance tomography in soft tissue tumors [in German]. *Orthopade.* 1988;17:134–142.
- Gomaa MA, Hammad MS, Abdelmoghy A, Elsherif AM, Tawfik HM. Magnetic resonance imaging versus computed tomography and different imaging modalities in evaluation of sinonasal neoplasms diagnosed by histopathology. *Clin Med Insights Ear Nose Throat.* 2013;6:9–15.
- Schmidt GP, Reiser MF, Baur-Melnyk A. Whole-body MRI for the staging and follow-up of patients with metastasis. *Eur J Radiol.* 2009;70:393–400.
- Nensa F, Beiderwellen K, Heusch P, Wetter A. Clinical applications of PET/MRI: current status and future perspectives. *Diagn Interv Radiol.* 2014;20:438–447.
- Antoch G, Bockisch A. Combined PET/MRI: a new dimension in whole-body oncology imaging? *Eur J Nucl Med Mol Imaging.* 2009;36(suppl 1):S113–S120.
- Buchbender C, Heusner TA, Lauenstein TC, Bockisch A, Antoch G. Oncologic PET/MRI, part 1: tumors of the brain, head and neck, chest, abdomen, and pelvis. *J Nucl Med.* 2012;53:928–938.
- Buchbender C, Heusner TA, Lauenstein TC, Bockisch A, Antoch G. Oncologic PET/MRI, part 2: bone tumors, soft-tissue tumors, melanoma, and lymphoma. *J Nucl Med.* 2012;53:1244–1252.
- Biederer J, Beer M, Hirsch W, et al. MRI of the lung (2/3). Why ... when ... how? *Insights Imaging.* 2012;3:355–371.
- Sommer G, Koenigkam-Santos M, Biederer J, Puderbach M. Role of MRI for detection and characterization of pulmonary nodules [in German]. *Radiologie.* 2014;54:470–477.
- Biederer J, Hintze C, Fabel M. MRI of pulmonary nodules: technique and diagnostic value. *Cancer Imaging.* 2008;8:125–130.
- Rauscher I, Eiber M, Furst S, et al. PET/MR imaging in the detection and characterization of pulmonary lesions: technical and diagnostic evaluation in comparison to PET/CT. *J Nucl Med.* 2014;55:724–729.

17. Chandarana H, Heacock L, Rakheja R, et al. Pulmonary nodules in patients with primary malignancy: comparison of hybrid PET/MR and PET/CT imaging. *Radiology*. 2013;268:874–881.
18. Sommer G, Tremper J, Koenigkam-Santos M, et al. Lung nodule detection in a high-risk population: comparison of magnetic resonance imaging and low-dose computed tomography. *Eur J Radiol*. 2014;83:600–605.
19. Baraliakos X, Listing J, von der Recke A, Braun J. The natural course of radiographic progression in ankylosing spondylitis—evidence for major individual variations in a large proportion of patients. *J Rheumatol*. 2009;36:997–1002.
20. American Joint Committee on C. *AJCC Cancer Staging Handbook: From the AJCC Cancer Staging Manual*. 7th ed. New York, NY: Springer; 2010.
21. Cistaro A, Lopci E, Gastaldo L, Fania P, Brach Del Prever A, Fagioli F. The role of <sup>18</sup>F-FDG PET/CT in the metabolic characterization of lung nodules in pediatric patients with bone sarcoma. *Pediatr Blood Cancer*. 2012;59:1206–1210.
22. Dabrowska M, Krenke R, Korczynski P, et al. Diagnostic accuracy of contrast-enhanced computed tomography and positron emission tomography with <sup>18</sup>-FDG in identifying malignant solitary pulmonary nodules. *Medicine (Baltimore)*. 2015;94:e666.
23. Opoka L, Kunikowska J, Podgajny Z, et al. Accuracy of FDG PET/CT in the evaluation of solitary pulmonary lesions: own experience. *Pneumonol Alergol Pol*. 2014;82:198–205.
24. Yilmaz F, Tastekin G. Sensitivity of <sup>18</sup>F-FDG PET in evaluation of solitary pulmonary nodules. *Int J Clin Exp Med*. 2015;8:45–51.
25. Farid K, Poullias X, Alifano M, et al. Respiratory-gated imaging in metabolic evaluation of small solitary pulmonary nodules: <sup>18</sup>F-FDG PET/CT and correlation with histology. *Nucl Med Commun*. 2015;36:722–727.
26. Khalaf M, Abdel-Nabi H, Baker J, Shao Y, Lamonica D, Gona J. Relation between nodule size and <sup>18</sup>F-FDG-PET SUV for malignant and benign pulmonary nodules. *J Hematol Oncol*. 2008;1:13–20.
27. Bar-Shalom R, Valdivia AY, Blaufox MD. PET imaging in oncology. *Semin Nucl Med*. 2000;30:150–185.
28. Regier M, Kandel S, Kaul MG, et al. Detection of small pulmonary nodules in high-field MR at 3 T: evaluation of different pulse sequences using porcine lung explants. *Eur Radiol*. 2007;17:1341–1351.
29. Schäfer JF, Vollmar J, Schick F, et al. Detection of pulmonary nodules with breath-hold magnetic resonance imaging in comparison with computed tomography [in German]. *Rofo*. 2005;177:41–49.
30. Biederer J, Schoene A, Freitag S, Reuter M, Heller M. Simulated pulmonary nodules implanted in a dedicated porcine chest phantom: sensitivity of MR imaging for detection. *Radiology*. 2003;227:475–483.
31. Rakheja R, DeMello L, Chandarana H, et al. Comparison of the accuracy of PET/CT and PET/MRI spatial registration of multiple metastatic lesions. *AJR*. 2013;201:1120–1123.
32. Biederer J, Graessner J, Heller M. Magnetic resonance imaging of the lung with a volumetric interpolated 3D-gradient echo sequence. *Rofo*. 2001;173:883–887.
33. Müller NL, Gamsu G, Webb WR. Pulmonary nodules: detection using magnetic resonance and computed tomography. *Radiology*. 1985;155:687–690.
34. Kauczor HU, Kreitner KF. Contrast-enhanced MRI of the lung. *Eur J Radiol*. 2000;34:196–207.
35. Keshamouni VG, ed. *Lung Cancer Metastasis: Novel Biological Mechanisms and Impact on Clinical Practice*. New York, NY: Springer; 2009.
36. Kennecke H, Yerushalmi R, Woods R, et al. Metastatic behavior of breast cancer subtypes. *J Clin Oncol*. 2010;28:3271–3277.